GFZ
Helmholtz-Zentrum
POTSDAM

Originally published as:

Geissler, W. H., Jokat, W. (2004): A geophysical study of the northern Svalbard continental margin. - Geophysical Journal International, 158, 1, pp. 50—66.

DOI: http://doi.org/10.1111/j.1365-246X.2004.02315.x

Geophys. J. Int. (2004) **158,** 50–66 doi: 10.1111/j.1365-246X.2004.02315.x

A geophysical study of the northern Svalbard continental margin

Wolfram H. Geissler[1,*] and Wilfried Jokat[2]

[1] *TU Bergakademie Freiberg, Institute of Geophysics, Gustav-Zeuner-Strasse* 12, D-09599 *Freiberg, Germany. E-mail: wgeiss@gfz-potsdam.de*
[2] *Alfred Wegener Institute for Polar and Marine Research, Columbusstrasse,* D-27515 *Bremerhaven, Germany*

Accepted 2004 March 6. Received 2004 February 25; in original form 2001 December 3

SUMMARY

In the summer of 1999, the first systematic seismic profiles were acquired across the northern Svalbard continental margin east of 15°E. Approximately 1470 km of multi-channel seismic reflection data as well as sonobuoy wide-angle data were collected up to 82°N. With few exceptions the signals imaged the whole sedimentary cover down to the acoustic basement. The uppermost sedimentary deposits of the inner shelf yield *P*-wave velocities of 2 km s^{-1} and higher, indicating erosion and compaction due to a former ice load. The inner shelf east of Hinlopen Strait has only a thin veneer of over-consolidated sediments above the acoustic basement. Beneath the outer shelf, up to 3.5 km of sedimentary deposits cover the down-faulted acoustic basement. The continental slope is heavily eroded due to bottom current activity and slumping. At about 30°E the morphology of the continental slope has a smooth appearance. Shelf progradation only in the vicinity of glacial troughs crossing the shelf (associated with submarine fans) indicates main sediment transport by ice streams during former glacial periods. The maximum sedimentary thickness in the Sophia Basin is more than 9 km, and the Nansen Basin has a sediment thickness of 4.5 km close to the margin. Gravity modelling along the seismic profiles was performed to constrain the position of the continent–ocean transition. Existing sedimentary thickness and structural maps were extended over the area investigated. The new data provide no evidence for the presence of former extensive subaerial volcanic sequences (seaward-dipping reflectors), which would have been emplaced during the break-up along the margin. Thus, we consider this part of the margin as non-volcanic.

Key words: Arctic, continental margins, Eurasia Basin, reflection seismology, seismic stratigraphy, Svalbard.

INTRODUCTION

The northern Svalbard continental margin is part of the Eurasian margin of the Arctic Ocean (Fig. 1). The Cenozoic development of this margin began when seafloor spreading in the Eurasia Basin started in the earliest Tertiary and caused the separation of the Lomonosov Ridge from the Barents/Siberian shelves. This is documented by aeromagnetic measurements (Karasik 1968; Vogt *et al.* 1979), which show a pronounced magnetic anomaly pattern interpreted as seafloor spreading anomalies in the Eurasia Basin. Chron 24 is the oldest identified anomaly (Karasik 1974; Vogt *et al.* 1981). However, in an area between chron 24 and the Eurasian continental slope, the type of underlying crust is unknown. Seafloor spreading probably started some million years earlier than indicated by chron 24 (Vogt *et al.* 1979; Sundvor & Austegard 1990; Jokat *et al.* 1995). Latest some 20 Ma after the initial break-up, a volcanic plateau formed in the westernmost part of the Arctic. The area of excessive volcanism was separated by subsequent seafloor spreading processes around chron 13 (Feden *et al.* 1979). Today the two parts are named the Morris Jessup Rise and Yermak Plateau, respectively.

The Yermak Plateau lies at the transition between the former sheared western and the rifted northern Svalbard continental margins. A dense grid of seismic reflection lines exists up to 81°30′N in this area, but the crustal fabric of the plateau is still under debate. On the basis of aeromagnetic studies (Feden *et al.* 1979) and seismic investigations (Jackson *et al.* 1984), it is suggested that the plateau has a dual origin. South of 82°N it might consist of stretched continental crust, whereas the northern part might be composed of oceanic-type crust. This northernmost segment, together with the Morris Jessup Rise, was probably formed by extensive volcanism at a former triple junction north of Svalbard before chron 13 (Jackson *et al.* 1984). The history of sediment deposition is poorly known. The oldest drilled sediments sampled by the Ocean Drilling Program (ODP) Leg 151 (Sites 910–912; Myhre *et al.* 1995) were Pliocene in age (Thiede *et al.* 1995; Hull *et al.* 1996).

Owing to ice conditions in the High Arctic, but especially north of Svalbard, almost no geophysical data exist east of 15°E to describe the continent–ocean transition (COT) and the break-up

*Now at: GeoForschungsZentrum Potsdam, Telegrafenberg, D-14473 Potsdam, Germany.

 © 2004 RAS

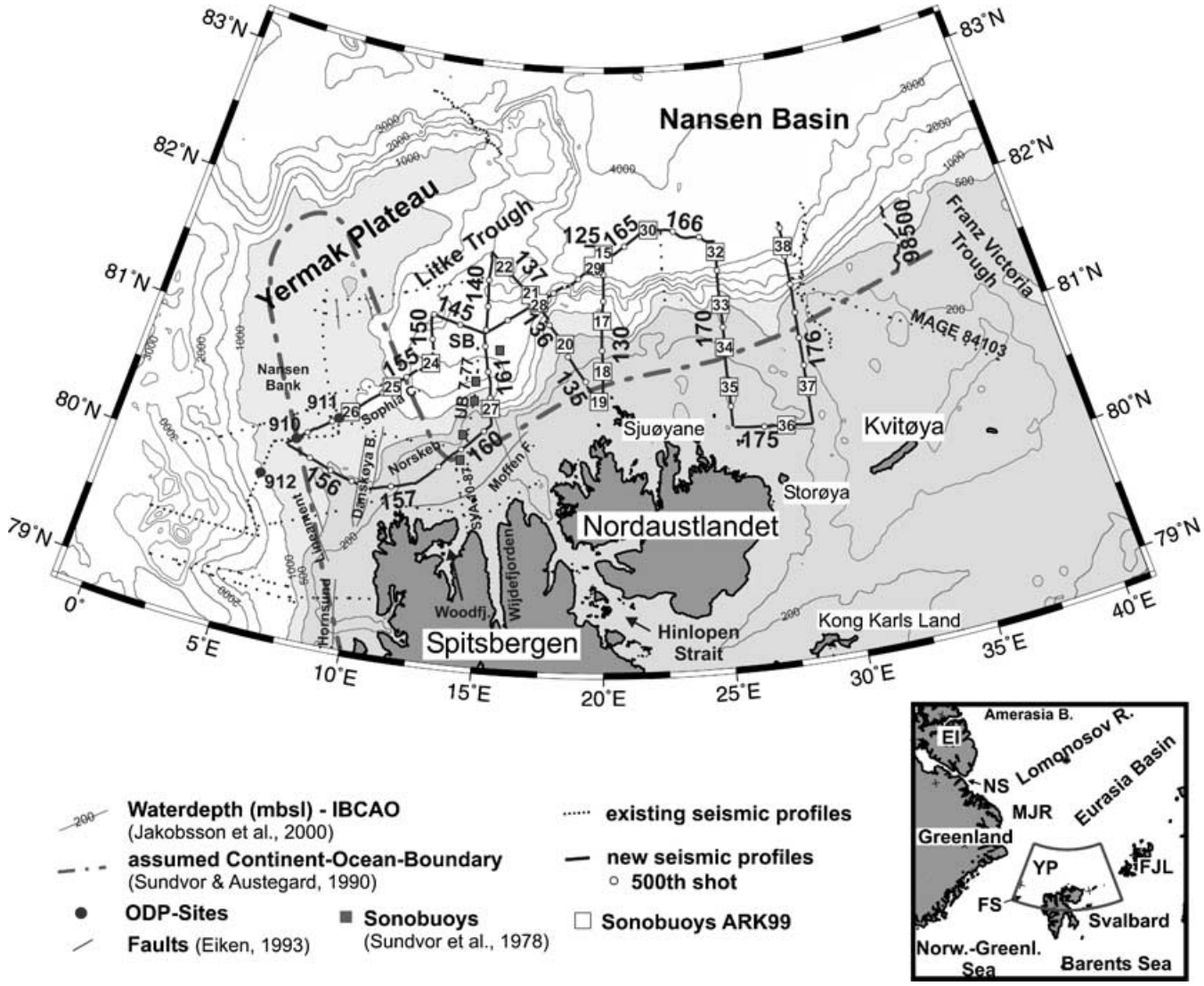

Figure 1. Map of the area investigated along the northern Svalbard continental margin. Bold lines display the profiles acquired during expedition ARKTIS-XV/2 of RV *Polarstern* 1999. Some of the existing, older profiles (Jackson *et al.* 1984; Eiken 1994; Weigelt 1998) are drawn as dotted lines. The names of the profiles were abbreviated to make the figure more readable (e.g. 166 denotes AWI-99166). The same was done for the sonobuoys (e.g. 19 denotes SB9919). Black circles mark the ODP sites from Leg 151 (Myhre *et al.* 1995). IBCAO bathymetry is taken from Jakobsson *et al.* (2000). The dashed line represents the assumed continent–ocean boundary according to Sundvor & Austegard (1990). Danskøya B.—Danskøya Basin, EI—Ellesmere Island, FJL—Franz Josef Land, FS—Fram Strait, Moffen F.—Moffen Fault, MJR—Morris Jessup Rise, Norskeb.—Norskebanken, NS—Nares Strait, SB—Sophia Basin, Sophia C.—Sophia Canyon, Woodfj.—Woodfjorden, YP—Yermak Plateau.

processes between the Lomonosov Ridge and the Barents Sea/Siberian shelves. Very few seismic reflection profiles cross the continental margin (Eiken 1994; Baturin *et al.* 1994), and only along one profile was sufficient recording time chosen to image basement structures in the Nansen Basin close to the margin. In the summer of 1999, an exceptionally wide polynya north of Svalbard permitted the acquisition of new seismic reflection data between 15°E and 30°E. The data were acquired to the northern rim of the polynya with a 2600-m long streamer. Systematic bathymetry and seismic investigations between 5°E and 30°E up to 82°N (Fig. 1) were carried out (Jokat 2000), along with gravity and some aeromagnetic measurements. In addition, sonobuoys (SB) were deployed along the seismic profiles to provide better constraints on the seismic velocities both within the sedimentary column and especially within the basement beneath the shelf. Here, we present the results of the interpretation of these data, which provide the first insight into the fabric of the northern Svalbard continental margin.

DATA ACQUISITION, PROCESSING AND MODELLING PROCEDURE

About 1470 km of marine multichannel seismic data were acquired using a 24-liter airgun cluster. The signals were recorded by a streamer (96 channels, group spacing 25 m) with an active length of 2400 m and a maximum offset of 2600 m. The shooting interval was 15 s, resulting in a mean shot distance of 40 m. During profiling, no sea-ice disturbed the measurements. Along almost all profiles the seismic signals revealed the top of acoustic basement. Some profiles contain data gaps caused by ship track variations arising

from helicopter starts and landings. The processing of the reflection data included frequency filtering, velocity analysis, stacking (fold 40–60), velocity filtering to suppress multiple reflections, and time migration in the fx-domain.

21 sonobuoys were launched to determine the seismic velocities for the sedimentary strata and the underlying crust. The wide-angle data from sonobuoys were processed and modelled using the programs ZPLOT (Zelt 1998; Sroda 1999) for phase picking and identification, and RAYINVR (Zelt & Smith 1992) for modelling the velocity structure. The algorithm for the program RAYINVR is the numerical solution of the ray-tracing equation after Červeny *et al.* (1977). The first step was to calculate 1-D models; the second was to establish 2-D models that included the results from the steep-angle measurements. Problems occurred where we could not detect a clear basement reflection in the steep-angle data. In these cases, the basement reflector/refractor was modelled, like deeper discontinuities, as a horizontal boundary. To estimate the resolution of the final models we conducted a parameter test for layer boundaries and velocities as proposed by Zelt & Smith (1992). We perturbed one parameter within the assumed time uncertainty of ± 0.05 to ± 0.10 ms and kept the other parameters constant. The maximum deviation from the final model was used as an estimate of the accuracy: it was ± 0.2 km s^{-1} for velocities and 200 m for depths. The information from the sonobuoys was used to convert the two-way traveltime (TWT) of the basement reflector to depth in order to produce the sediment thickness map.

To constrain the location of the COT, gravity data acquired with the seismic profiles were used for forward modelling. The information from the seismic measurements about sedimentary thickness was used as model input to calculate the gravity effect along crustal transects. We estimated the density of the sedimentary strata from the seismic velocities using the Gardner equation (Gardner *et al.* 1974). As the calibration for our gravity modelling we assumed a Moho depth of 25 km north of Spitsbergen, according to Austegard & Sundvor (1991) and Czuba *et al.* (1999). Model parameters from the end of one profile were used as model input for the beginning of the following profile.

RESULTS

The distribution of the seismic lines and their observed structures will be described here. In addition, seismic stratigraphic models will be introduced for certain areas. Whenever possible, we used the nomenclature of existing stratigraphic models. We divided the sedimentary column into units based on the seismic velocity–depth functions derived from sonobuoy measurements and the seismic pattern/reflection character along the multichannel seismic profiles. The results of the modelling of the wide-angle data are compiled in Fig. 2. Details of the velocity–depth functions will be discussed, together with the appropriate seismic reflection profiles. Since no deep seismic refraction data exist across the northern margin of Svalbard, little is known about its crustal structure. Here, the seismic velocities from the sonobuoys are used to constrain the upper crustal structure. In a first approach, the structural information from the seismic steep and wide-angle data is used to constrain a first-order gravity model.

Southern Yermak Plateau

On the southern Yermak Plateau (profile AWI-99155; Fig. 3), three seismic units (YP-1, YP-2 and YP-3) have been defined by Eiken & Hinz (1993). Unit YP-1 consists mostly of parallel layers and infill of grabens. *P*-wave velocities range from 2.4 up to 4.2 km s^{-1}. Unit YP-2 consists of a thick sequence of subparallel continuous reflectors and has its greatest thickness at the southwestern end of profile AWI-99155. To the northeast (shotpoint 1750) this unit thins rapidly before it becomes thicker again. *P*-wave velocities for unit YP-2 from sonobuoy measurements range between 1.9 and 2.4 km s^{-1}. The boundary to the overlying unit YP-3 represents in the southwest an erosional discordance. Unit YP-3 has a transparent reflection character with some continuous reflectors beneath the top of Yermak Plateau (Nansen Bank). Farther to the northeast, YP-3 is an acoustically fine-layered sequence. Unit YP-3 shows minimum thickness beneath the top of Yermak Plateau (Fig. 3a; shotpoint 2700). It thickens towards the southwest as well as in the northeast. *P*-wave velocities in the unit are between 1.7 and 1.8 km s^{-1}. The correlation of the seismic units across profile AWI-99155 is difficult due to 3-D effects, such as off-line reflections (shots 400 to 1200), as the line runs along the strike of the Sophia Canyon. Faults in the basement are clearly visible on the southern Yermak Plateau. *P*-wave velocities within the basement of Yermak Plateau are 5.0 km s^{-1} (SB9926) and 4.6 km s^{-1} (SB9925). The latter value correlates reasonably well with results from former investigations in that area (e.g. Myhre *et al.* 1982).

Danskøya Basin

The N–S striking Danskøya Basin is situated between the mainland and the southern Yermak Plateau (Figs 1 and 4). We divided the sedimentary column here into three seismic units, namely DB-1, DB-2 and DB-3 (DB—Danskøya Basin). DB-1 within the centre of the basin comprises subparallel reflectors; in the deeper parts a more transparent character is observed. The seismic velocities range between 2.8 and 4.2 km s^{-1}. Unit DB-2 contains some internal parallel reflections, and *P*-wave velocities range from 2.0 to 2.7 km s^{-1}. Unit DB-3 has a transparent character with only some continuous reflectors. At the eastern end of profile AWI-99157 (Fig. 4; shots 750 to 900) the thickness of the unit decreases strongly. Units DB-2 and DB-3 continue beneath Norskebanken to the east. Farther to the northwest the basement becomes more irregular, meaning that locally the basement is not well defined (Fig. 4; line AWI-99156, shots 600 to 1000). Between shots 100 and 600 a crustal basement block cuts through the sedimentary section. The faults at the top of the crustal block cut through the entire unit DB-2.

Norskebanken

At the northern termination of Hinlopen Strait and Woodfjorden (Fig. 1), previous seismic profiles SVA 10-87/UB 7-77 show a well-developed prograded shelf (Eiken 1994). The sequences probably represent glacial sediments deposited during repeated advances and retreats of the Svalbard ice shield. The new line AWI-99161 just to the east of this location shows an unusual shape of the continental slope (Fig. 5), with a prominent slump scarp on the continental slope. Cherkis *et al.* (1999) described in detail this region of massive slumping, probably late Quaternary in age, on the basis of sidescan sonar data.

The acoustic basement beneath the shelf is not imaged along line AWI-99161 (Fig. 5a) or line AWI-99160 (Fig. 4) because of strong seafloor multiples. The observed sedimentary thickness is at least 3 km. Sundvor *et al.* (1978) and Eiken (1994) reported sedimentary deposits up to 4 km thick beneath Norskebanken. Following

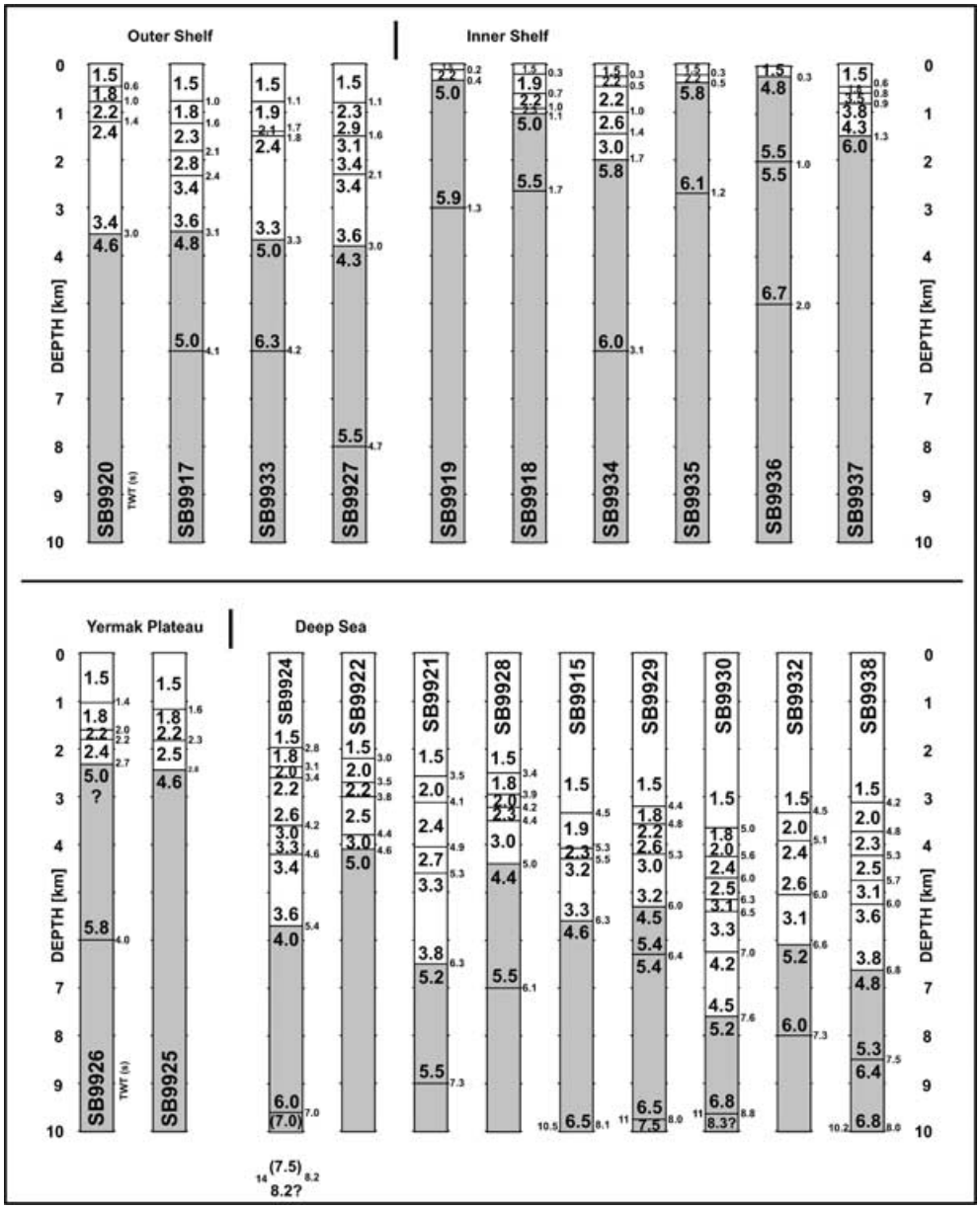

Figure 2. *P*-wave velocity–depth functions (v_p in km s^{-1}) from sonobuoy measurements. Grey shading indicates the assumed basement velocities. In the reflection data near SB9924 and SB9927 we could not detect a clear basement reflector.

Eiken (1994) we divide the sedimentary column into two seismic units, namely NoB-1 and NoB-2 (NoB—Norskebanken; NB-1/-2 of Eiken; Figs 4 and 5). NoB-1 has interval velocities above 3 km s^{-1}; for unit NoB-2 the velocities range between 2.3 and 2.5 km s^{-1}. NoB-2 has a maximum thickness of 1500 m near the shelf-break and thins towards the deep sea (Fig. 5a). Beneath the continental rise a transparent and discontinuous reflection pattern exists. These events were named the 'fuzzy reflector' by Sundvor *et al.* (1978). The nature of this reflector is speculative, since no drilling information is available in the area. As on the existing profile, additional reflectors are visible down to 5 s TWT. Because of strong seafloor multiples and signal scattering in the uppermost sediments, no reflections from the basement are visible in the southern part of the Litke Trough.

Sophia Basin

East of the Yermak Plateau (start of line AWI-99155, Fig. 3a) the uppermost sediments are acoustically fine layered. Eastwards along lines AWI-99140 and AWI-99165 the seafloor is more irregular (Figs 5a and 6). Peaks up to 200 m high (above seafloor) are visible in the seismic section (Fig. 6c). These non-typical elevations and the rough seafloor cause strong diffractions that mask the seismic signals from deeper sedimentary strata and the acoustic basement in this region. Some kilometres to the west on profile AWI-99145, the acoustic basement reflector is observed down to about 7.7 s TWT (Fig. 6b). Here, the sedimentary thickness reaches about 9 km (5 s TWT), calculated from stacking velocities. A nearby sonobuoy measurement from Sundvor *et al.* (1978; in Jackson 2000) can also

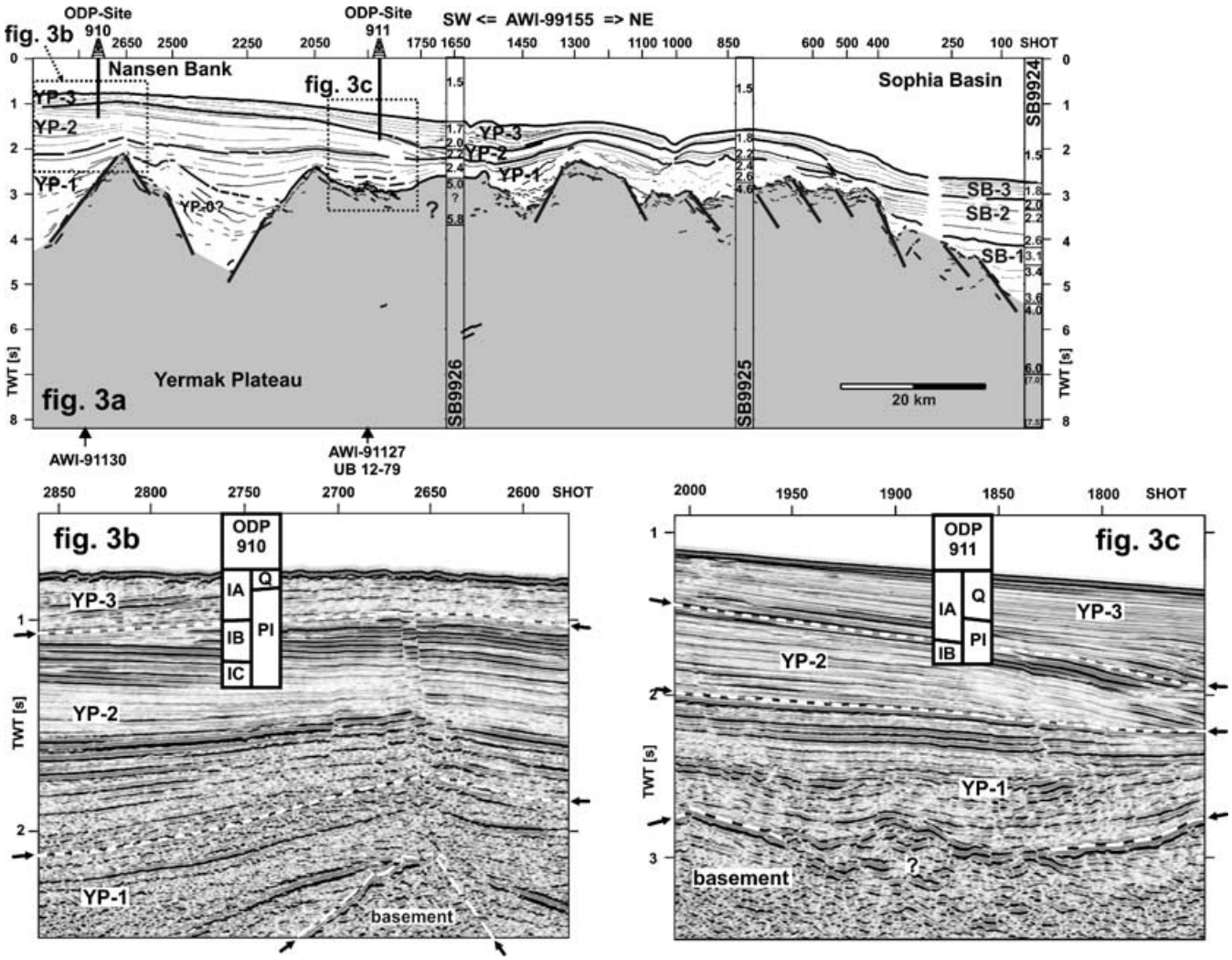

Figure 3. (a) Profile AWI-99155 (line drawing) with seismic velocities from sonobuoys. Sedimentary rocks may be present beneath the opaque basement reflector in the seismic reflection data. SB9924 to SB9926 show the seismic velocities (in km s^{-1}) obtained by ray tracing of wide-angle data. (b) Correlation of seismic units with the results of ODP-910C. The information about the lithological boundaries is taken from Shipboard Sci. Party (1995a). The more transparent reflection character of YP-3 compared with the underlying YP-2 may be caused by coarser material within YP-3. Bright reflections in the upper part of YP-2 might indicate the presence of gas, observed in the drill-hole (Stein *et al.* 1995). (c) Correlation of the seismic units with the results of ODP-911A. The lithological information about the drilled section is taken from Shipboard Sci. Party (1995b). Bright reflections in the upper part of YP-2 might indicate the presence of gas (Stein *et al.* 1995).

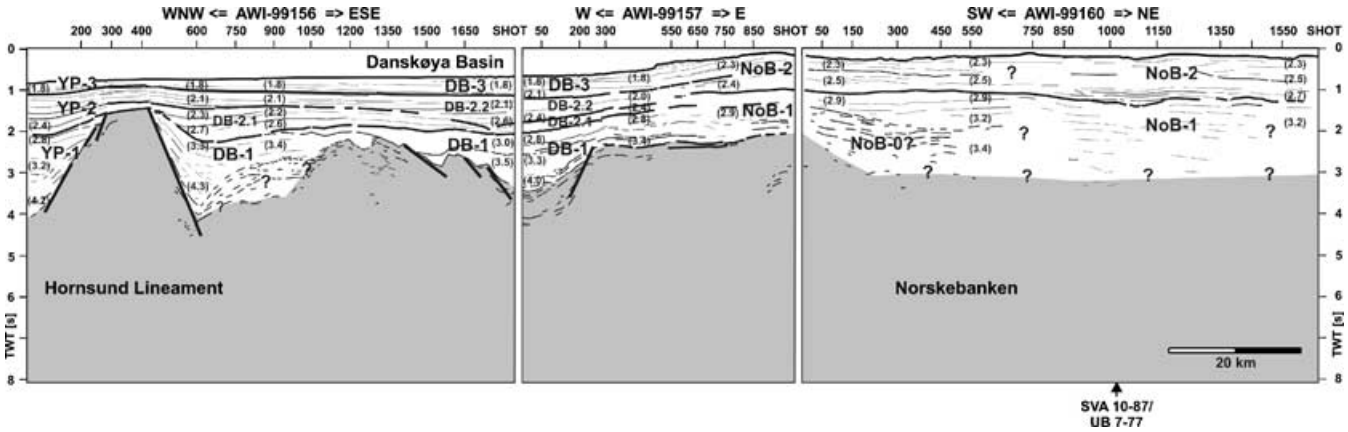

Figure 4. Line drawing of the seismic profiles AWI-99156-99157-99160 from the Hornsund lineament across Danskøya Basin to Norskebanken. Strong seafloor multiples mask the deeper sedimentary structure beneath Norskebanken. Values in parentheses are the interval velocities (in km s^{-1}) obtained from stacking velocity analysis.

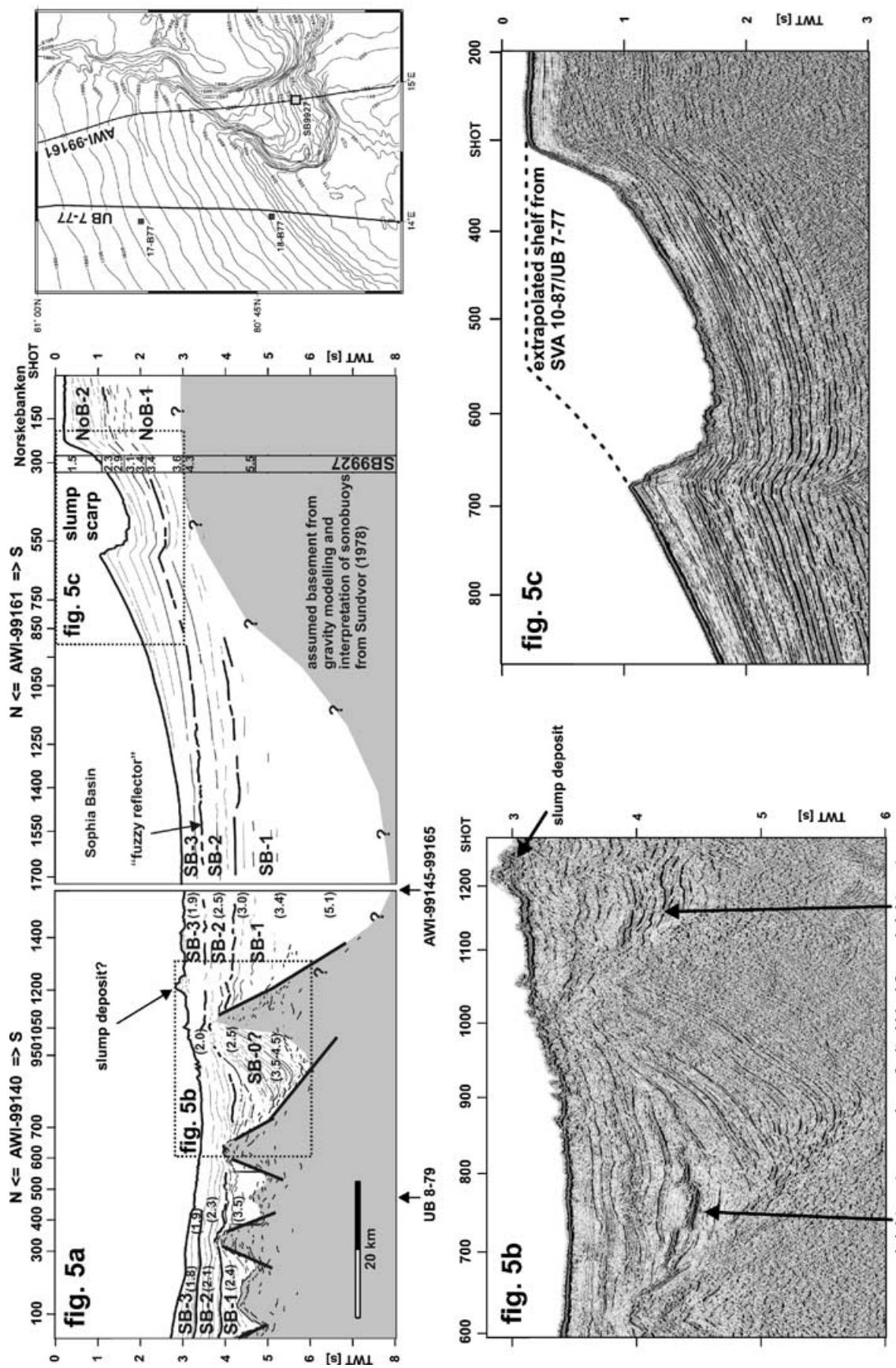

Figure 5. (a) Line drawing of the seismic profiles AWI-99140-99161 north of Spitsbergen. The basement in the southern part is not imaged by the seismic reflection data, but inferred from gravity modelling and sonobuoy measurements of Sundvor *et al.* (1978). SB9927 (at shot point 300 of line AWI-99161) shows the seismic velocities (in km s^{-1}) obtained by ray tracing of wide-angle data. Values in parentheses are the interval velocities (in km s^{-1}) obtained from stacking velocity analysis. For abbreviations see text. The inset map in the upper right corner shows the location of the seismic profile relative to the slump area. Bathymetry modified after Cherkis *et al.* (1999). (b) Down-faulted block at the northern rim of Sophia Basin. The irregular seafloor topography between shots 900 and 1200 is caused by deposits of large-scale slumps. Several bright spots can be observed in the vicinity of Sophia Basin, possibly representing magmatic sills and/or accumulations of natural gases/fluids. (c) Slide scar at the outermost shelf north of Spitsbergen (part of profile AWI-99161). The slump was directed to the east. The dotted line indicates the assumed original shape of the shelf break adopted from line SVA 10-87/UB 7-77.

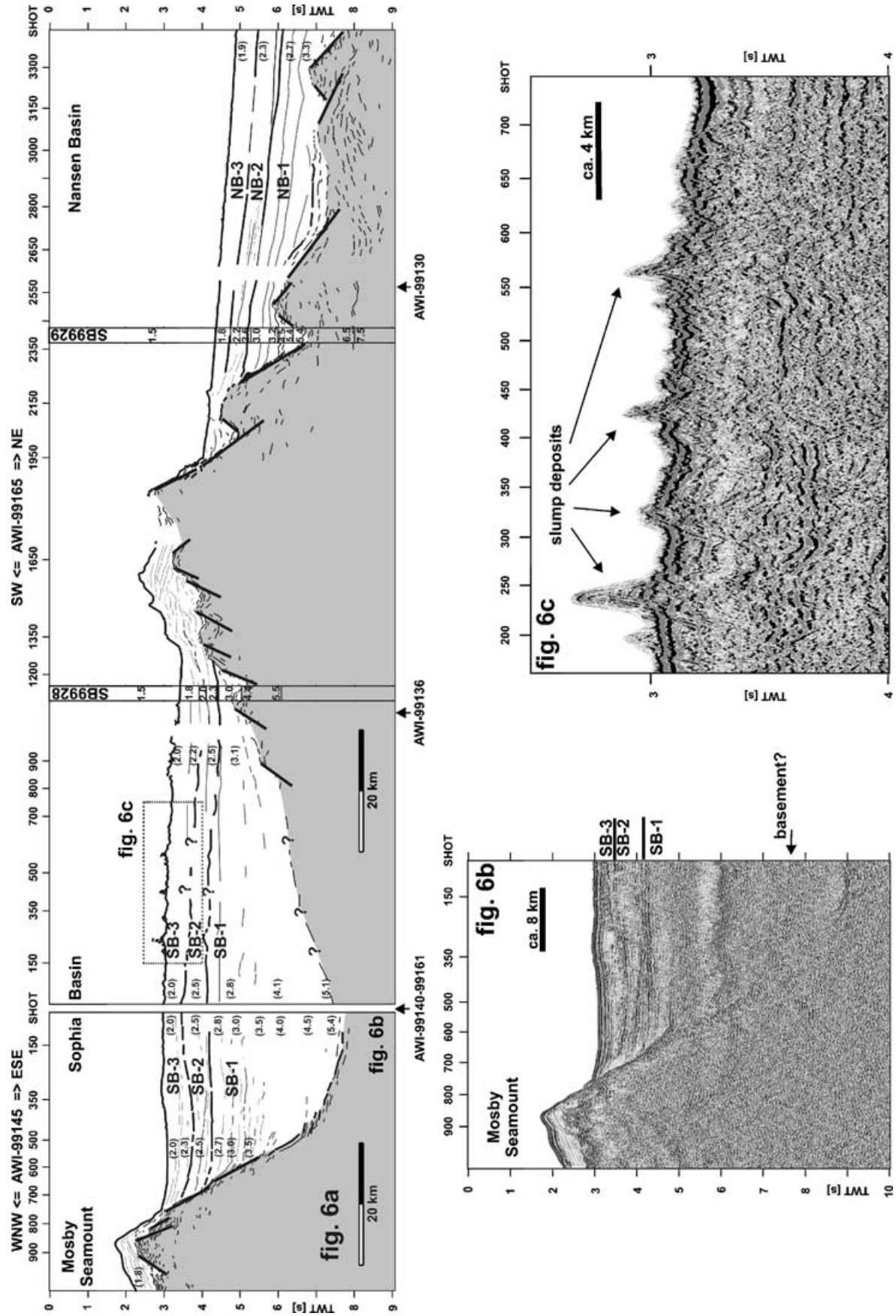

Figure 6. (a) Line drawing of the seismic profiles AWI-99145-99165 from the flank of Mosby Seamount across Sophia Basin towards Nansen Basin. Values in parentheses are the interval velocities (in km s^{-1}) obtained from stacking velocity analysis. (b) From the flank of Mosby Seamount we can follow the acoustic basement down to about 7.7 s TWT. Sophia Basin has up to 9 km infill of sediments. (c) Seafloor topography within the Sophia Basin/Litke Trough interpreted as slump deposits. Some of these structures rise to 200 m above the adjacent seafloor. The sedimentary structure beneath the seafloor is not well resolved due to strong diffractions.

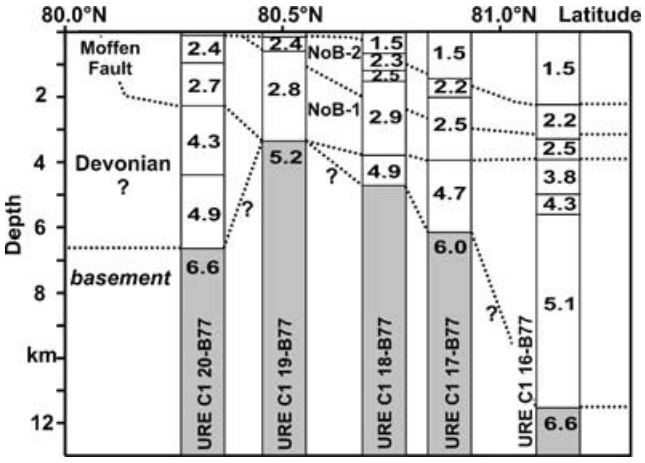

Figure 7. Interpretation of results of sonobuoy measurements from Sundvor *et al.* (1978; in Jackson 2000) north of Spitsbergen along the profiles SVA 10-87/UB 7-77 and AWI-99161. For location of this sonobuoy profile see Fig. 1.

be interpreted in this way (Fig. 7; 16-B77). We name this thick sedimentary accumulation the Sophia Basin. The sedimentary column of this basin is divided into three units, namely SB-1, SB-2 and SB-3 (SB—Sophia Basin; Figs 5 and 6a). SB-3 is built up by 400 m thick (0.4 s TWT) acoustically fine-layered sediments at the basin margin and by slump deposits at the top. *P*-wave velocities are between 1.8 and 2.1 km s^{-1}. The base of SB-3 is at 3.2 to 3.4 s TWT. Unit SB-2 contains a more chaotic (transparent and discontinuous) reflection pattern and shows *P*-wave velocities between 2.3 and 2.5 km s^{-1}. SB-2 is bounded from the underlying sequence SB-1 in some places by strong reflections at 4.2 s TWT. SB-1 also shows internal reflectors, but we did not subdivide this unit. At a depth of 11 km the *P*-wave velocities are about 5 km s^{-1}.

North of Sophia Basin, the acoustic basement is irregular (profiles AWI-991137/99140; Figs 5 and 8), and the basement reaches to the seafloor (Fig. 8). A seamount rises to a minimum water depth of 1500 m. It coincides with a small positive magnetic anomaly reported by MacNab & Verhoef (1995). In the vicinity of the newly discovered seamount basement *P*-wave velocities are about 5.0 to 5.2 km s^{-1} (SB9921, SB9922). On profile 99140 (Fig. 5b; shots 700 to 1200) a faulted basement block is imaged.

North of Nordaustlandet

Two structural boundaries can be identified north of Nordaustlandet: the hinge zone between the inner and outer shelf; and a system of normal faults beneath the continental slope. The seismic data on the inner shelf show no or only thin sediments overlying the acoustic basement (Fig. 9). The sedimentary strata have *P*-wave velocities above 1.9 km s^{-1}. These relative high velocities indicate erosion and/or compaction due to a former ice sheet. Beneath the outer shelf the sedimentary thickness is 3 to 3.5 km at maximum. This drastic increase in sedimentary thickness is associated with down-faulted basement (e.g. AWI-99170, Fig. 10a). The dislocation along these faults, which have an apparent dip of about 20°, reaches values up to 2000 m. The basement topography beneath the outer shelf is highly variable. In some parts it is heavily faulted (Fig. 9a, shotpoint 900–1900 of line AWI-99130), while on profile AWI-99170 (Fig. 10a, shotpoint 800–1950) a relatively smooth and strong basement reflector is visible. The sedimentary section beneath the outer shelf can be divided into three seismic units (Fig. 9c), namely NA-1, NA-2 and NA-3 (NA—Nordaustlandet). The lower unit NA-1, about 1000 m thick, appears mostly transparent. Only some continuous reflections are visible. The boundary towards the overlying seismic unit is an angular unconformity. The acoustically well stratified sedimentary strata of NA-2, which are up to 1500 m thick, rest with an onlap on the acoustic basement and partly on unit NA-1. NA-3 (about 400 to 500 m thick) rests conformably on unit NA-2 and shows continuous reflections in the lower part and a partly transparent character in the upper part. The seafloor is disturbed by channels and/or iceberg plough marks, which cut through the uppermost sediments. The boundary between NA-2 and NA-3 is not that clear. On the next line, 100 km to the east (AWI-99170), the uppermost deposits show prograding sequences at shotpoint 1600 (Fig. 10a). At about 30°E, another 60 km to the east, a thick sedimentary wedge can be identified on the outer shelf (line AWI-99176; Fig. 11). The sediments are situated at the mouth of a glacial trough east of Nordaustlandet. This sedimentary prism can be compared with similar structures in front of Woodfjorden and Hinlopen Strait and along the Western Svalbard and Barents Sea continental margins. Here the uppermost seismic

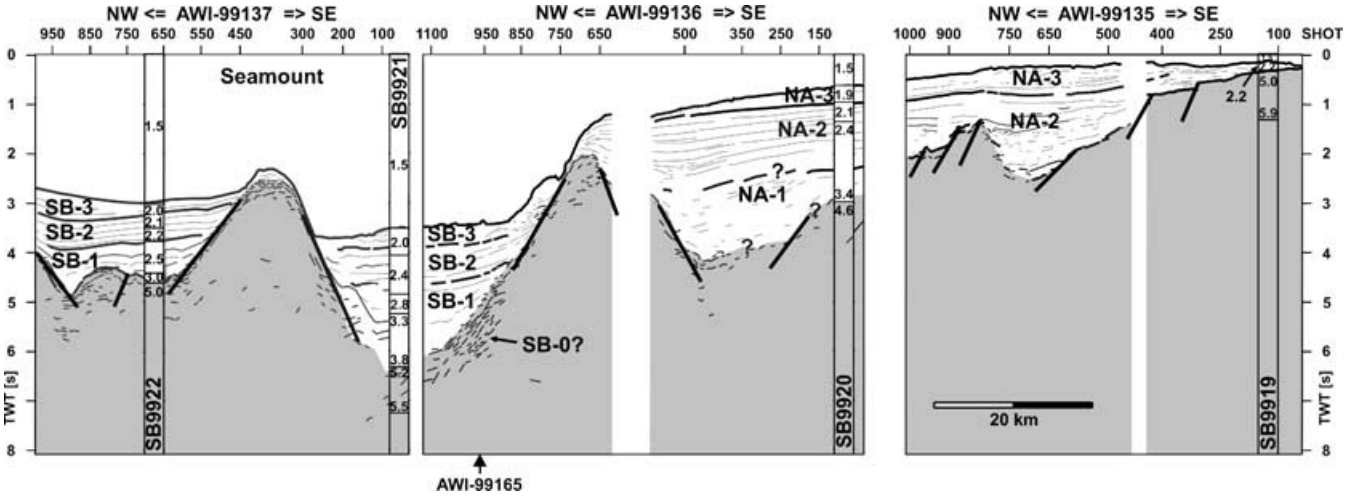

Figure 8. Line drawing of profiles AWI-99135-99136-99137 from the southern rim of the northeastern Yermak Plateau across the flank of a newly discovered seamount (Jokat 2000) towards the shelf north of Nordaustlandet. The channel between the seamount and the shelf is probably used by bottom water flows into Nansen Basin.

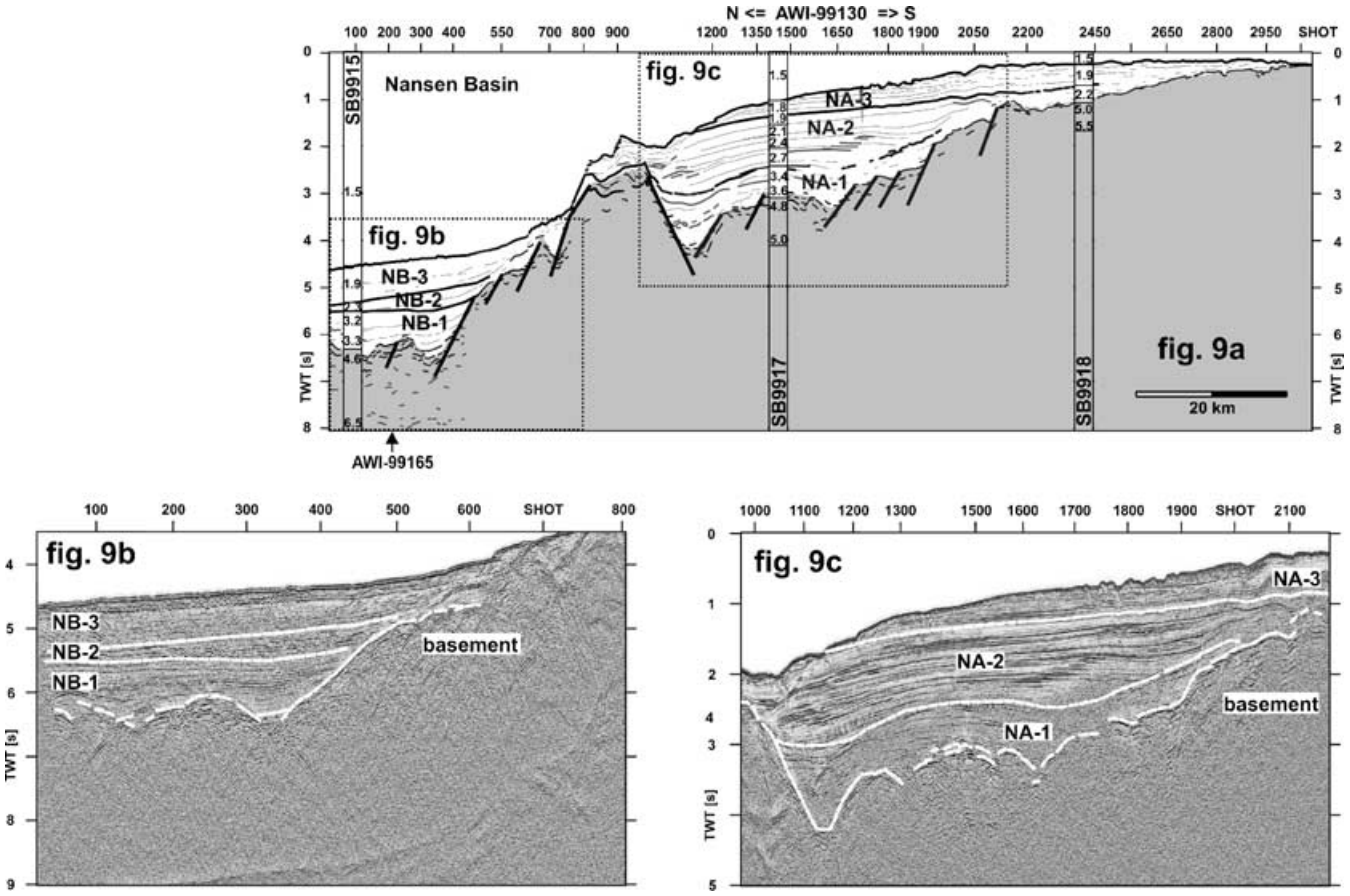

Figure 9. (a) Profile AWI-99130 (line drawing) at 20°E north of Nordaustlandet. (b) The rim of Nansen Basin north of Nordaustlandet. The sediments were subdivided into seismic units based on the reflection character and *P*-wave velocities. (c) Subdivision of seismic units beneath the outer shelf area north of Nordaustlandet.

unit KV-3 (KV—Kvitøya) is divided from unit KV-2 by a different reflection pattern. These prograding sequences within unit KV-3 are typical for glaciated continental margins at high latitudes (Bart & Anderson 1995). Repeated advances and retreats of glaciers/ice streams created this sedimentary prism. As on the other profiles, a relatively transparent seismic unit, KV-1, can be distinguished above the faulted acoustic basement.

The crustal transition to the deep Nansen Basin in the north is characterized by a system of normal faults beneath the continental slope (Figs 9, 10 and 11). The fault zone is between 15 and 20 km wide. Below the abyssal plain north of the continental margin, up to 4.5 km of sedimentary rocks rest on basement, which is probably of oceanic origin. Three seismic units can be distinguished (Figs 9, 10 and 11). The lower (up to 2500 m thick) unit NB-1 (NB—Nansen Basin) consists of continuous, parallel reflections. This unit onlaps the main boundary fault beneath the continental slope. NB-2 and NB-3 have a more transparent/chaotic reflection character, with some scattered continuous reflections. These units indicate the onset of massive slumping on the continental margin (Fig. 10b). The boundary between these two seismic units is not everywhere clear, because of the discontinuous reflections. Both units seem to thicken towards the east. The thickening is related to the submarine fan in front of the northern termination of the glacial trough at 30°E.

For the inner shelf north of Nordaustlandet and Kvitøya, *P*-wave velocities of 4.8 to 6.0 km s^{-1} within the acoustic basement are modelled from sonobuoy data. Similar velocities are calculated from refracted waves in the shot-gathers. Beneath the outer shelf *P*-wave velocities range from 4.6 to 5.0 km s^{-1}, whereas the basement velocities in the deep-sea basin vary between 4.4 and 5.2 km s^{-1}.

STRATIGRAPHY

We used existing stratigraphic models for most of the regions investigated. Since the old seismic data sets on which the models are based were not available for our interpretation, a direct comparison and/or revision of the models was not possible. In Fig. 12 we show a preliminary stratigraphic correlation of the northern Svalbard continental margin. Our seismic correlation is mainly based on marker horizons, sedimentary thicknesses, reflection character, and *P*-wave velocities. The age and composition of the units are constrained by the results of ODP sites 909–911 (Shipboard Sci. Party 1995a,b; Thiede *et al.* 1995) and 986 (Forsberg *et al.* 1999). Note that only sparse age data and tie lines exist to better constrain the interpretation.

Starting in the west, we used the age information from the existing ODP drill-site 911, which is based on biostratigraphy and palaeomagnetics. Site 911 is located on the flat southern part of Yermak Plateau (Figs 1 and 3c). The base of the lithological subunit IA (360 mbsf), which can be correlated with the base of seismic unit YP-3, has an age of approximately 2.6 Ma (Shipboard Sci. Party 1995b). According to Shipboard Sci. Party (1995b) and Thiede *et al.* (1995), the average Pliocene deposition rate at this drill-site is about

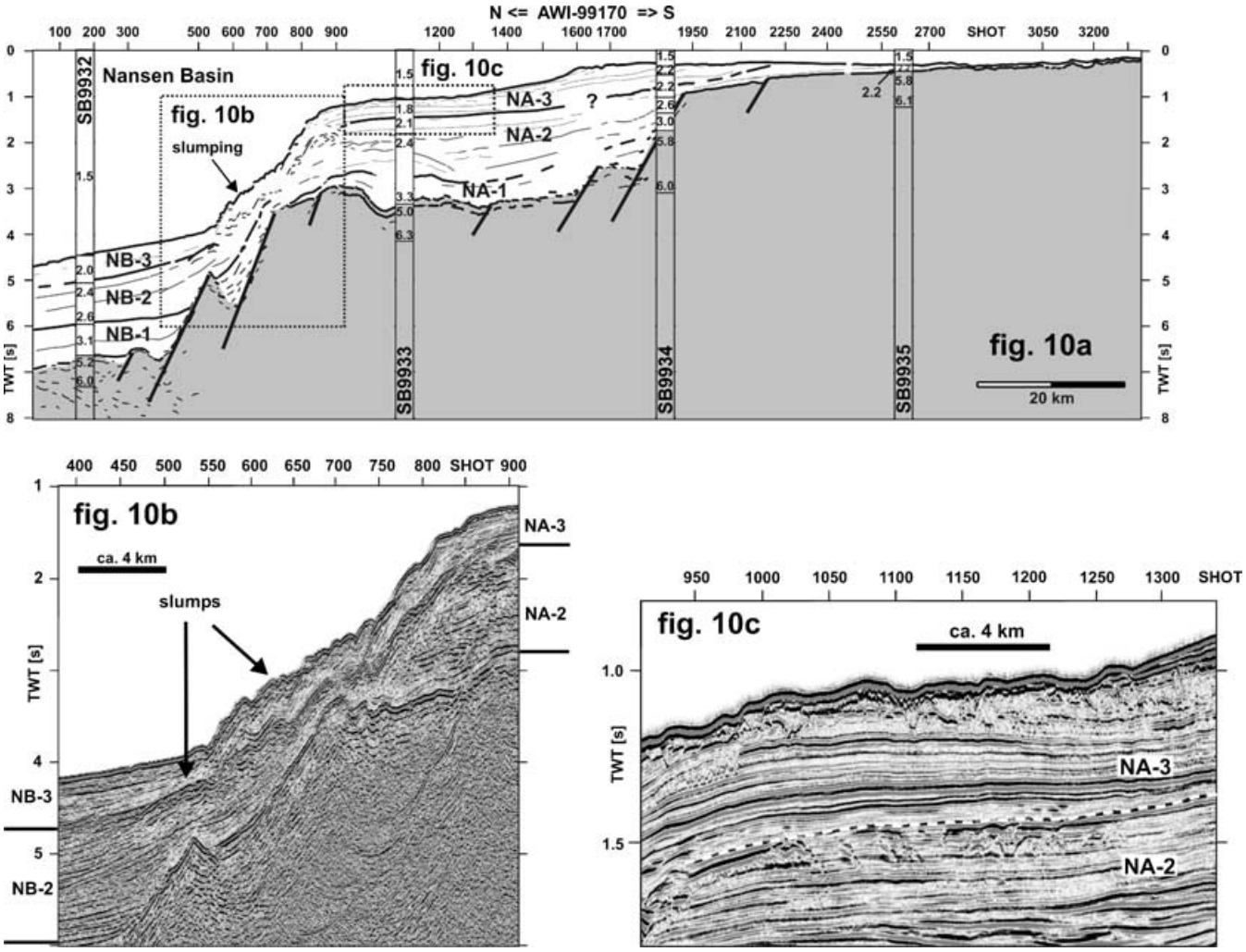

Figure 10. (a) Profile AWI-99170 (line drawing) at 26°E north of Nordaustlandet. (b) Intensive slumping at the continental slope north of Nordaustlandet. (c) Subdivision of seismic units beneath the outer shelf area north of Nordaustlandet.

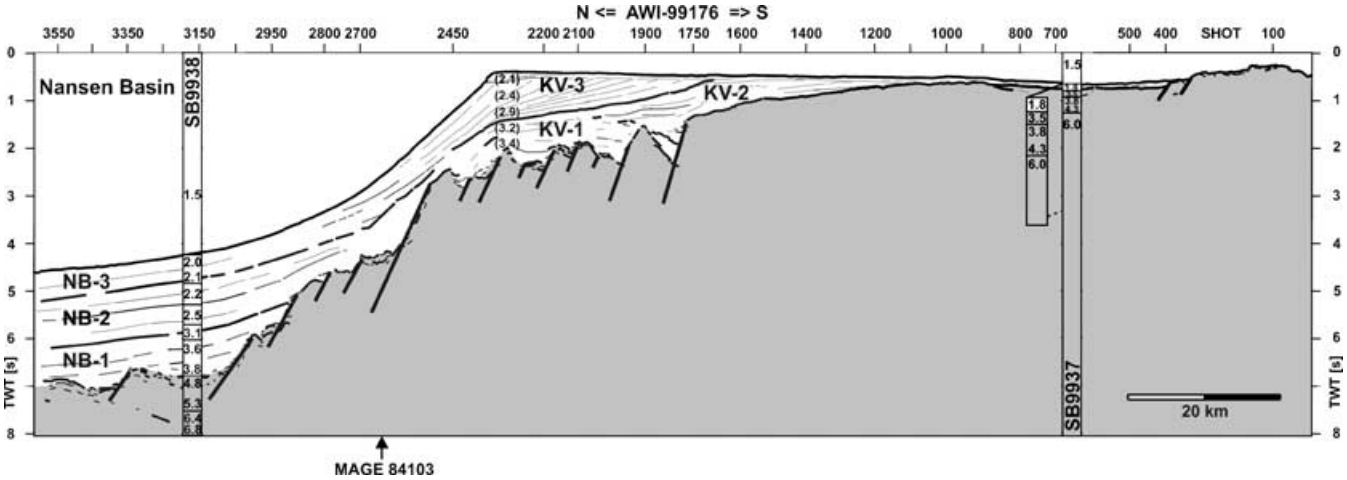

Figure 11. Line drawing of seismic profile AWI-99176 at 30°E north of Nordaustlandet. Shelf progradation occurs in front of a glacial trough between Nordaustlandet and Kvitøya.

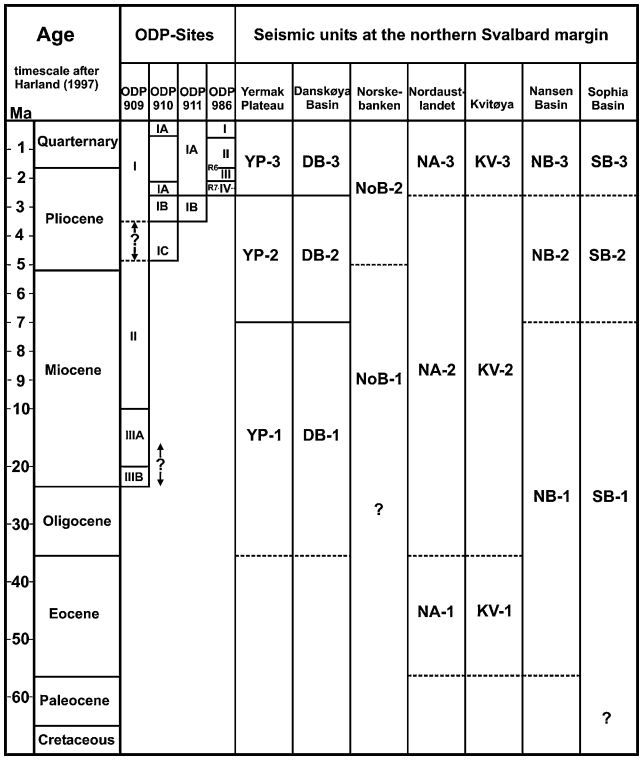

Figure 12. Stratigraphic models for the area investigated. Information on the ODP drill-holes 909–911 and 986 was taken from Thiede *et al.* (1995) and Forsberg *et al.* (1999), respectively. Hull *et al.* (1996) provided some age revisions, especially at site 909, based on biostratigraphy. Seismic reflectors R6 and R7, drilled by ODP-986, are regional reflectors below the western Svalbard continental margin (Faleide *et al.* 1996).

17 cm ka^{-1}, and the sediments at the bottom of the drill-hole (506 mbsf) have an age of about 3.5 Ma. Seismic profile AWI-99155 (Fig. 3) shows that the base of unit IB at site 910 (Shipboard Sci. Party 1995a) correlates with the bottom of drill-hole 911 and therefore with the base of the lithological unit IB at this site (Fig. 12).

Beneath the drilled section at site 911, there exists an additional 1400 m of sedimentary strata above the acoustic basement (Fig. 3, 300 m of unit YP-2, 1100 m of unit YP-1). Because YP-2 thins beneath the drill-site, we chose a slightly decreased sedimentation rate of 10 cm ka^{-1} for YP-2, and calculated an age of 6–7 Ma for the base of YP-2. Assuming the same sedimentation rate we obtained an age of 18 Ma for the base of YP-1. A lower sedimentation rate of only 5 cm ka^{-1} implies an age of 35 Ma for the oldest sedimentary rocks. The base of the lithological unit IC at site 910 should have an age of 4–5 Ma at maximum (Fig. 12).

On Yermak Plateau and north of Nordaustlandet the uppermost sediments show a transparent reflection character. Here, we can correlate the uppermost seismic unit YP-3 (Fig. 3b) with glacial-marine sediments, which are characterized by a high incidence of dropstones (subunit IA, Shipboard Sci. Party 1995a,b).

The information from the drill-holes and the seismic properties have been used to constrain the age of the units of Danskøya Basin, Norskebanken and Nordaustlandet. Thus we correlated the glacial-marine fans at the mouth of two large fjords off northern Spitsbergen, the Hinlopen Strait (upper part of NoB-2) and east of Nordaustlandet (KV-3), with YP-3. The fans were possibly deposited by ice streams/glaciers, which probably originated on Svalbard. The base of the seismic unit NoB-2 correlates more or less with the base of the lithological unit IC at ODP site 910, and therefore has an age of 4–5 Ma at maximum. The boundary between seismic units DB-2.1 and DB-2.2 should be between 5 and 6 Ma.

The 'fuzzy reflector' (Sundvor *et al.* 1978) along line AWI-99161 (uppermost part of SB-2) can be interpreted as the top of sandy debris flows resulting from mass movements. Such deposits, with a chaotic reflection pattern and similar seismic velocities, were drilled at the western Svalbard continental margin at ODP site 986 (Forsberg *et al.* 1999). These sediments, possibly indicating the onset of glaciation, are bounded by the regional seismic reflectors R6 and R7 (Faleide *et al.* 1996) that were dated to about 1.6 and 2.3 Ma, respectively (Forsberg *et al.* 1999). If these seismic reflectors were to correlate strongly with observed reflectors at the northern Svalbard margin, this would imply a younger age for the uppermost two seismic units (SB-3/2, NB-3/2); however, seismic correlation along the western margin shows that deposits from mass movements vary both vertically (in time) and laterally (Faleide *et al.* 1996). Butt *et al.* (2000) concluded from the ODP site 986 results that glaciation did not reach the shelf-break of western Svalbard before 1.6 Ma. If our age correlation along the northern margin with the results of ODP sites 910 and 911 on the Yermak Plateau is correct this implies possibly different glacial histories along the northern and western Svalbard continental margins.

YP-2 can be directly correlated with DB-2 at the intersection of two profiles. The correlation of YP-2 with SB-2 is more problematic because of the complex seafloor topography within the Sophia Canyon. However, YP-2 should correlate more or less with SB-2 and NB-2. The above estimated age (6–7 Ma, upper Miocene) of the base of YP-2 is also assumed for the other correlated units. The seismic units YP-2, DB-2 and SB-2 show some indications (e.g. mounds) of bottom current activity. It could be that the onset of the current activity is connected with the development of the deep-water passage through the Fram Strait (see also Eiken & Hinz 1993).

The base of the deeper units YP-1/DB-1 and NA-2/KV-2 is assumed to be 35 Ma old, based on an average sedimentation rate of 5 cm ka^{-1} for these units. This average sedimentation rate can be estimated by dividing the average sedimentary thickness at the margin (3 km) by the overall sedimentation period (60 Ma). The base of units NA-1, KV-1 and NB-1 should have an age of approximately 55–60 Ma according to the beginning of seafloor spreading in the Eurasia Basin. No constraints exist on the ages of the bases of NoB-1 and SB-1. The huge sedimentary thickness of the Sophia Basin might be a hint that sedimentation in this part of the continental margin had already started during the Cretaceous, maybe in a local rift/pull-apart structure.

CONSTRAINTS ON THE CRUSTAL STRUCTURE OF THE CONTINENTAL MARGIN BASED ON GRAVITY DATA

The observed free-air anomaly ranges from −20 mGal to +120 mGal in the investigated area north of Spitsbergen. A prominent gravity high exists at the mouth of Hinlopen Strait (Fig. 13a, see also Faleide 1995). This could be caused by the combination of a complex 3-D structure of the seafloor (edge effect) in the region of massive slumping and a dense intrusion within the crust. For the 2-D gravity models, a lower crust with a density of 2.85 g cm^{-3} is normally assumed. In the central Sophia Basin we modelled a Moho depth of only 15 km, assuming a crustal density of 2.9 g cm^{-3} (Fig. 13a). The crustal thickness would be only 4 km, covered by 9 to 10 km of sedimentary rock.

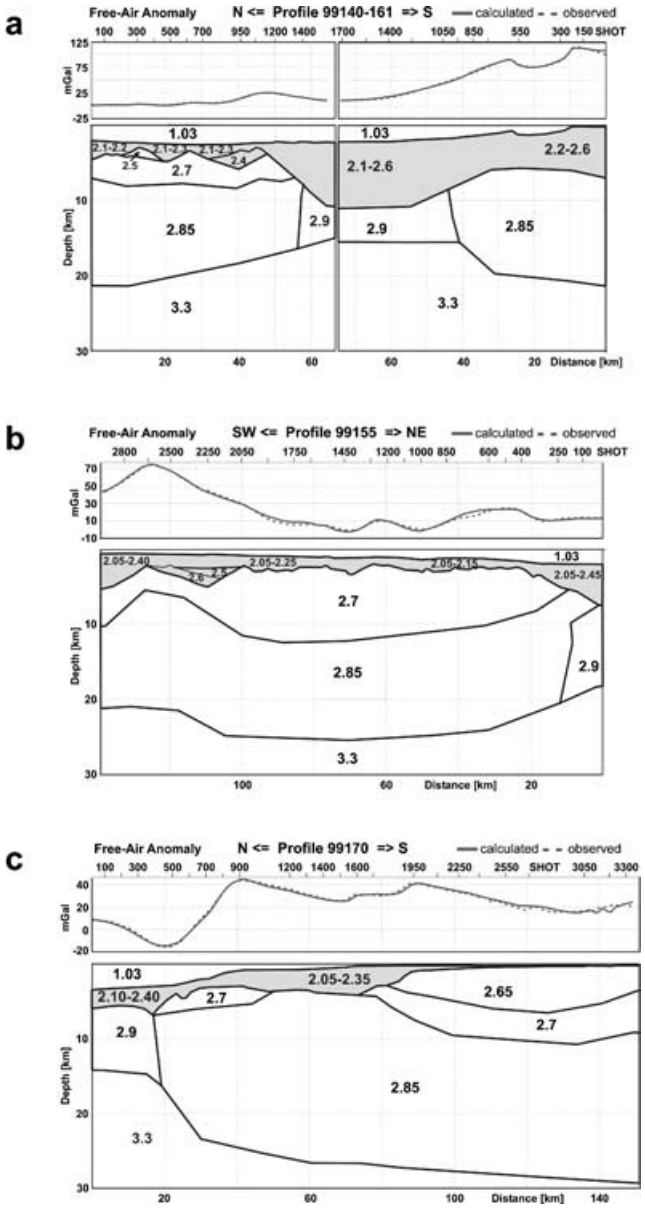

Figure 13. (a) Gravity model along lines AWI-99140-99161 (density in 10^3 kg m^{-3}). The free-air anomaly (scale in mGal or 10^{-5} m s^{-2}) was modelled for each profile individually. (b) Gravity model along line AWI-99155 (density in 10^3 kg m^{-3}). (c) Gravity model along line AWI-99170 (density in 10^3 kg m^{-3}).

Towards the southwestern Yermak Plateau the modelled Moho depth decreases to values slightly above 20 km beneath the Hornsund lineament (Fig. 13b). The gravity high of about +70 mGal at the western rim of the southern Yermak Plateau is explained by a combination of reduced crustal thickness and high-density intrusions into the upper crust of the plateau. For the central part of the Yermak Plateau we modelled a Moho depth of about 25 km (Fig. 13b).

The free-air anomaly north of Nordaustlandet ranges between −40 and +90 mGal. A prominent anomaly with its maximum above the shelf-break and its minimum above the continental rise indicates a structural boundary (Fig. 13c). Water depth and sedimentary rocks alone cannot explain the observed gravity anomaly. In our model this anomaly is associated with a prominent shallowing of the crust–mantle boundary from 25–27 km depth beneath the outer shelf to about 15 km depth beneath the continental rise.

INTERPRETATION AND DISCUSSION

The continental slope and the outer shelf between 15°E and 30°E are highly affected by erosion/slumping (Fig. 10b). Bathymetry data obtained by Cherkis *et al.* (1999) show deeply incised canyons along the continental margin. These authors reported the existence of a large-scale mass wasting along the continental margin in front of Hinlopen Strait. This feature was also investigated with profile AWI-99161 (Fig. 5). The slide scarps extend down-slope from water depths of 160 m to more than 2000 m. Approximately 220 km^3 of sediments were removed in front of the Hinlopen Strait (Cherkis *et al.* 1999). The seismic and the bathymetry data suggest that the slide scar is not a recent structure. The feature is located in front of a deep glacial trough, which is a pathway for transport of material by ice streams to the shelf edge. Thus, mass wasting might have begun with the onset of glacial-marine sedimentation in this area and continued with repeated slumps until the Holocene. The slumped sediments were deposited in the adjacent deep sea. Rough seafloor topography in the Sophia Basin (Figs 5b and 6c) may be caused by debris and blocks from this sediment slide.

The total thickness of sedimentary rocks north of Svalbard is highly variable. We used the sedimentary thickness map of Austegard & Sundvor (1991) mainly for the area west of 15°E, and added new information for the region between 15°E and 30°E to compile a more complete map of sedimentary thickness at the northern Svalbard continental margin (Fig. 14a). On the southern Yermak Plateau, a sedimentary section up to 5 km thick is observed within graben-like structures. The graben-infill is difficult to interpret. It might contain marine as well as terrestrial sediments that were deposited during the early rift phases between Greenland and Svalbard. Identical sedimentary thicknesses have been found on previous profiles (Austegard & Sundvor 1991; Eiken 1994). Within the Sophia Basin the sedimentary thickness probably reaches more than 9 km (Fig. 14a). Both seismic and gravity data (Figs 6b, 7 and 12) support this estimate. However, the deeper sedimentary and crustal structure of the basin is not well constrained. We speculate that this basin might be a feature that already existed in Late Cretaceous times during the early rift phases between the Eurasian and Greenland plates. The Sophia Basin might be one of the first extensional basins to have formed during the opening of the Eurasia Basin.

Approximately 4 km of Cenozoic sedimentary rocks are present beneath the Spitsbergen shelf west of 15°E (Sundvor *et al.* 1978; Eiken 1993, 1994). In contrast, only a relatively thin sedimentary veneer exists north of the Nordaustlandet coast, thickening to a maximum value of 1 km at the hinge zone (Fig. 10a, shotpoint 1950). In our stratigraphic interpretation, these sediments are mainly marine-glacial deposits of Late Cenozoic age. The new seismic lines indicate only a thin sedimentary sequence beneath the slope and the deeply incised canyons. The easternmost line AWI-99176 shows the presence of prograding glaciomarine sequences, which were deposited during advances and retreats of glaciers/ice streams. To some extent, this is also true for line AWI-99161 northwest of the Hinlopen Strait. Apart from those data, no large slope aprons (associated with glacial trough mouth fans) developed along the margin between 15°E and 30°E (almost 300 km). This assumption is reinforced by the swath bathymetry data acquired between the seismic profiles. Bart & Anderson (1995) suggested that significant slope propagation occurs when the ice sheet grounds for relatively long periods of

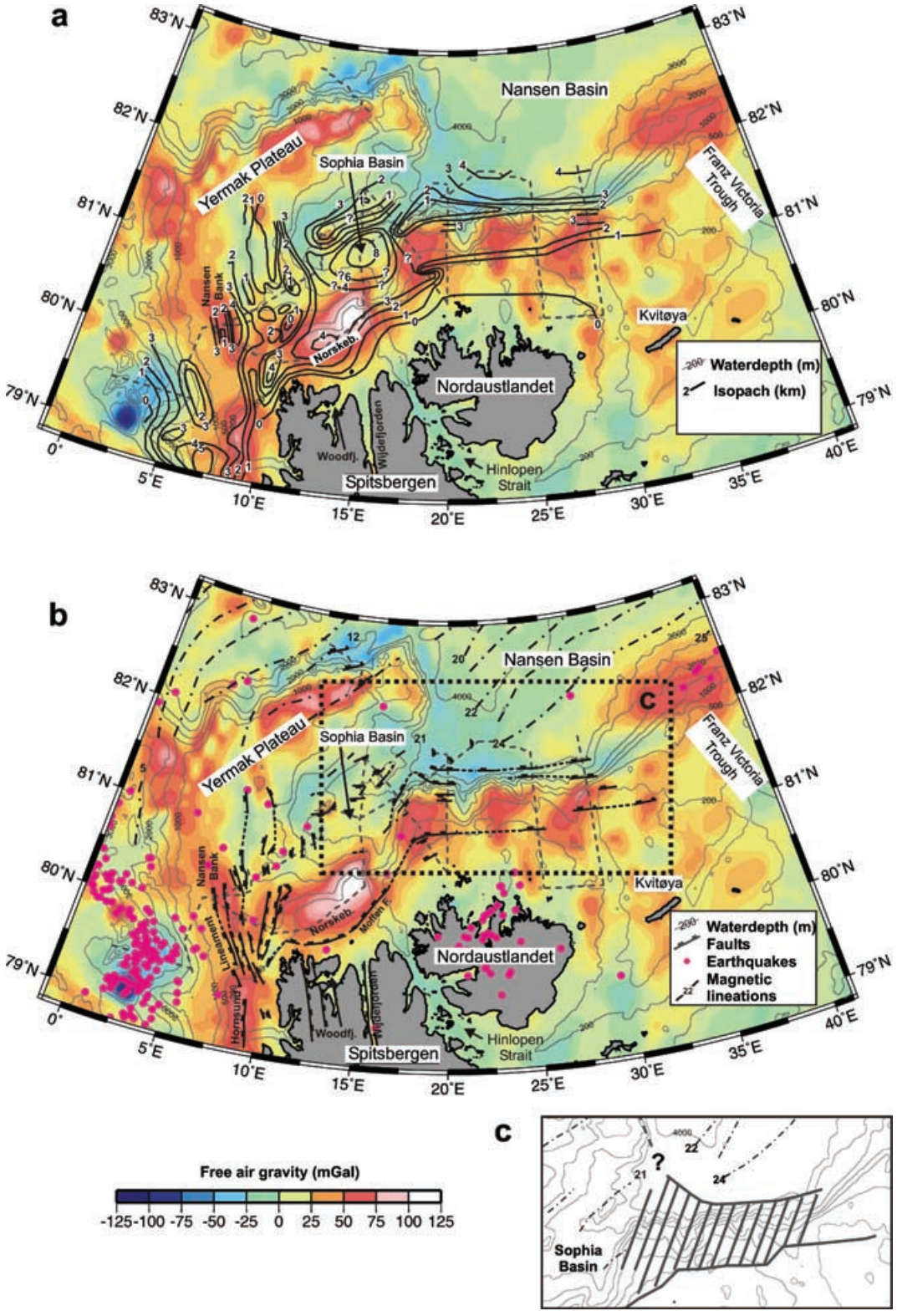

Figure 14. (a) Distribution of sediments below the northern Svalbard continental margin. Isopachs are in km. The map includes data from Austegard & Sundvor (1991). The Arctic gravity grid is plotted in colour (free-air anomaly in mGal or 10^{-5} m s^{-2}). (b) Simplified structural map of the northern Svalbard continental margin on the basis of Eiken (1993, 1994) and Weigelt (1998). The major faults are marked. The black lines represent the magnetic lineations (Vogt *et al.* 1979). The Arctic gravity grid is plotted in colour to support our structural interpretation. The box marks the location of the inset (part c). (c) Location and width of the continent–ocean transition zone north of Nordaustlandet (hatched area). We did not extend our interpretation farther westwards, since no deep seismic data exist and therefore the nature of the crust is hypothetical.

time. Aggradation is the result of relatively short-lived grounding events that may or may not reach the shelf edge (Bart & Anderson 1995).

The sedimentary deposits along the northern Svalbard margin may be interpreted in a similar way. Ice streams, which created long-lived grounded ice tongues, generated the smooth topography of the continental slope east of 30°E. West of this longitude, the ice sheet received less material from the hinterland and thus may not have been grounded for long time periods and/or it did not move very far to the north. This might indicate that the ice sheet covering the areas south of the investigated margin (Nordaustlandet and northern Spitsbergen) was mainly drained at a few locations through ice streams. The ice sheet between these troughs may not have been thick enough to produce significant horizontal mass transport. However, enough melt water was present to create or maintain the rough topography of the continental slope. From the seismic data, it is not clear if the deep canyons along the margin were created during the glaciation of Svalbard, or if they are older. We prefer the latter interpretation. Our assumption is that greater glacial sediment input in the area west of 30°E would have created a similar slope topography to that seen on line AWI-99176 (Fig. 11). The part of the shelf that shows more sediment aggradation (Figs 8–10) might contain glacial sediments, which were not affected by erosional processes. The fine seismic stratification of unit NA-3 and parts of NA-2 beneath the outer shelf (Fig. 10; shots 900–1400) is interpreted as that here fine sediments were deposited beneath a floating ice sheet during some time periods. The area is well below 700 m of water depth at the present day, and the seafloor shows evidence for iceberg plough marks (Figs 9c and 10c). These mostly undisturbed units might contain a complete record of the glacial history of Svalbard. A large glacial trough mouth fan occurs east of 35°E in the prolongation of the Franz Victoria Trough (Fig. 14a). Here, the gravity data suggest that the glacial fan extends well north of the 500 m isobath. Two additional seismic lines east of 30°E (98500, Jokat *et al.* 1999; 20010460, Jokat *et al.* 2002), which are not part of this study, support this interpretation.

The sedimentary section beneath the outer shelf (except for the Sophia Basin), east of 15°E, has a thickness of up to 3.5 km. In the Nansen Basin a maximum thickness of 4.5 km for the sedimentary rocks occurs at 82°N. This is the first reliable determination for the sediment thickness of the Nansen Basin close to the northern Svalbard continental margin. The deepest unit NA-1 contains, most likely, sedimentary rocks deposited during and after the early opening of the Eurasia Basin. Thick glacial accumulations of Late Cenozoic age do not appear to be present along the northern Svalbard–Barents Sea margin (with the exception of the Franz Victoria Trough area), while such deposits along the western Svalbard–Barents Sea continental margin reveal a thickness of 3–4 km (Fiedler & Faleide 1996).

The recently released Arctic gravity grid (http://164.214.2.59/GandG/agp/) shows four large positive gravity anomalies beneath the margin between 15°E and 30°E (Fig. 14). In this area none of these anomalies coincides with a large glacial trough mouth fan. Instead, the gravity anomalies more probably reflect the deeper structure of the northern margin of Svalbard. Only the lines AWI-99135 to AWI-99137 cross the centre of such a gravity high. Gravity modelling shows that this anomaly cannot be explained by the basement topography observed on the profiles. Most of the anomaly is a consequence of a density contrast at deeper levels, between the continental crust in the south and the rifted or oceanic crust in the north. It would especially useful to understand the nature of the gravity lows between the positive anomalies (Fig. 14). However, at the time of the survey the gravity grid was not available, and the survey was not designed to address it.

On the basis of the seismic data from this study and former investigations (Eiken 1993, 1994; Baturin *et al.* 1994; Weigelt 1998), we compiled a structural map of the continental margin (Fig. 14b), which will be described here. The southern Yermak Plateau is characterized by horst and graben structures. The acoustic basement (maybe older than 35 Ma) is masked locally by strong, opaque reflectors and is partly heavily faulted. These opaque reflectors possibly represent lava flows connected with extensive volcanism during the formation of the northern part of the plateau. There are indications from seismic and gravity data that, in some places, sedimentary deposits also rest beneath these reflectors. Some of the faults on the southern Yermak Plateau cut through the young sediments near the seafloor. At the seafloor, there are also indications of normal faulting in SeaMarc-II sidescan sonar images (Sundvor *et al.* 1991; Okay *et al.* 1991; Okay & Crane 1993). These probably deep-reaching faults, and sparsely occurring earthquakes (IRIS 2000) on the Yermak Plateau, point to recent crustal movements, which are connected with the evolution of the plate boundary along the Spitsbergen Fracture Zone. The high heat-flow values reported in that region (Crane *et al.* 1982; Jackson *et al.* 1984) are probably caused by active intrusive magmatism in the prolongation of the Knipovich Ridge (Okay & Crane 1993). Our gravity modelling supports previous assumptions (e.g. Jackson *et al.* 1984; Sundvor & Austegard 1990) that the southern part of the Yermak Plateau consists of thinned, approximately 20 to 25 km thick, continental crust. The continental nature of the crust is supported by a recent deep seismic sounding profile along the west coast of Spitsbergen up to almost 81°N (Ritzmann & Jokat 2003) and by the relatively weak magnetic anomalies over this area (Feden *et al.* 1979). Along the seismic refraction line a crustal thickness of approximately 22 km is reported, which fits reasonably well with our gravity modelling.

The basement was not imaged in seismic reflection data beneath the shelf north of Spitsbergen (11°E to 15°E) due to strong seafloor multiples. The basement here is probably down-faulted to about 4 km (Sundvor *et al.* 1978; Eiken 1994). The modelled average crustal density in this region is higher than in the adjacent shelf areas, suggesting that this part of the crust was heavily modified by mafic intrusions. Between the Yermak Plateau and the island of Spitsbergen, there is a narrow (40–50 km wide) basin, more than 11 km deep—the Sophia Basin. Beneath about 9 km of sedimentary rocks, we assume a relatively thin and dense crust with an affinity to oceanic crust. North of the Sophia Basin, at the southern rim of the northeastern Yermak Plateau we assume again thinned and modified continental crust from gravity modelling. Meta-sedimentary rocks with an affinity to rocks on the northern coast of Spitsbergen were dredged at the flank of a seamount (Hellebrand 2000). We speculate that possibly also large parts of the northern Yermak Plateau consist of former continental crust. We suggest that the observed high magnetic amplitudes along the northern Yermak Plateau are caused by intrusive and extrusive magmatic material.

Compared with geological structures north of Spitsbergen, the margin north of Nordaustlandet apparently exhibits a less complex structure. The uppermost crust shows seismic velocities (5 to 6 km s^{-1}) typical for normal crystalline continental crust. Seawards of the hinge line, the basement is down-faulted by more than 3 km. The crust beneath this outer shelf area probably has a transitional character, and can be distinguished from the continental crust by a higher average density, slightly reduced crustal thickness, and reduced

P-wave velocities in the upper part. A relatively smooth and strong basement reflector was observed along profile AWI-99170, which can be interpreted as a basaltic flow; however, no indications for seaward-dipping sequences could be found along the margin. The area of crustal thinning is about 80 to 100 km wide. Northwards, the transitional crust is bounded by an up to 20 km wide system of normal faults (Fig. 14). We assume that this fault system marks the transition to oceanic crust within the Nansen Basin. This assumption is supported by the results of gravity modelling in this study. The thickness of the oceanic crust in the Nansen Basin is about 5 to 8 km adjacent to the margin. The distance between the main boundary fault system on the line AWI-99176 and the first magnetic reversal (Fig. 14; chron 24) is about 50 km. Assuming a spreading half-rate of 1 cm a^{-1}, we calculate that spreading started about 5 Ma before chron 24.

The structure of the conjugate continental margin north of Spitsbergen and Nordaustlandet is important for the plate tectonic reconstruction of the northeastern Yermak Plateau. The existing seismic lines between 16°E and 20°E (Fig. 1) provide some constraints on this problem. The hinge line, named Moffen Fault (Eiken 1994), is displaced to the north by more than 100 km in the area of Hinlopen Strait. The northeastern Yermak Plateau is also about 100 km wide (2000-m isobath). The area between Moffen Fault and the assumed oceanic part of the plateau (Feden *et al.* 1979; Jackson *et al.* 1984; Sundvor & Austegard 1990) probably consists of thinned and heavily modified continental crust. In this way, most of the northeastern Yermak Plateau may be reconstructed to the continental margin without significant overlap. Then, the high-amplitude magnetic anomalies above the northern rim of the plateau can probably be explained by intrusions and basaltic flows, which were emplaced before or during the opening of Fram Strait and the separation of Yermak Plateau and Morris Jessup Rise. Consequently, the core of the Yermak Plateau might consist of heavily modified continental rocks. However, this implies a different extensional history for the Yermak Plateau in the parts west and east of the north–south running fault east of Nansen Bank (Fig. 14b) at the eastern margin of the plateau. New seismic refraction data (Ritzmann & Jokat 2003) indicate only minor extension for the southern plateau. East of the fault zone there might be a 50–100 km extended region at 15°E. Thus the fault zone might have been created by transtensional movements between the major part of the Yermak Plateau and its present-day northeastern tip. The new Arctic gravity grid (Fig. 14b) can be interpreted in such a way that this fault zone extends to 82°N and thus physically divides the plateau.

The tectonic processes active during the formation of the Eurasia Basin did not involve emplacement of thick volcanic sequences that can be identified as seaward-dipping reflectors. No such sequences are visible in the seismic data of this study. Such reflector sequences are thought to form through massive subaerial volcanism during break-up along volcanic margins. We cannot, however, exclude the presence of smaller volcanic complexes. The continent–ocean transition in the investigated area is characterized by down-faulted basement rocks, rather than by dipping volcanic sequences. This observation is supported by magnetic data (MacNab & Verhoef 1995), which do not show a strong anomaly along the margin that might point to volcanic material. Moreover, the gravity field does not show a continuous marginal anomaly. Instead, the mapped faults are associated with a strong, segmented gravity anomaly located within the continent–ocean transition zone. At least four distinct maxima are visible in the data, which might indicate zones of shallower basement and/or a density contrast between oceanic and rifted crust. The absence of large amounts of mafic material in the lower crust is also reported for the southern Yermak Plateau (Ritzmann & Jokat 2003). Thus, we consider the continental margin between 10°E and 30°E to be of the non-volcanic type. Deep seismic sounding profiles are needed in this area to make progress in understanding the tectonic evolution of this region and to confirm this interpretation.

CONCLUSIONS

The new seismic, wide-angle sonobuoy and gravity data presented here provide the first insight into the sedimentary and crustal structure of the northern Svalbard margin between 15°E and 30°E. East of 15°E, a maximum sedimentary thickness of 4.5 km has been determined in the Nansen Basin. The sedimentary cover below the continental shelf and slope is also highly variable in thickness, which ranges between 0 and 3 km. The data clearly indicate that the shape of the continental margin is highly variable in this region. In large areas, slumping and erosional processes within the sedimentary column dominate this margin. Here, the topography of the slope is quite rough. Shelf progradation is only evident in the vicinity of troughs crossing the shelf. The seismic data support the interpretation that the main sedimentary input into the Nansen Basin during the Late Cenozoic occurred along the glacial troughs of the ice streams. In between the troughs, local sediment transport processes connected with a minor amount of sediments dominate the shelf. Local gravity highs along the margin must have their origin in along-strike variations of the deeper crustal composition. The seismic profiles indicate that the anomalies are not consequences of huge glacial deposits.

There are significant structural differences between the margins north of Spitsbergen (affected by the evolution of the Yermak Plateau—diffuse rifting) and north of Nordaustlandet (normal rifting). The continent–ocean boundary north of Nordaustlandet is located farther to the north than previously assumed. The continent–ocean transition appears to be a zone approximately 100 km wide below the shelf. No magnetic anomalies are identified between Yermak Plateau and the continental margin of northern Svalbard. The crust within this zone probably consists of thinned and modified continental crust. This interpretation is supported by a dredge sample from the southern flank of the plateau, which represents a piece of continental rock.

Major continental boundary faults exist below the continental slope. The results of gravity modelling support the assumption that these faults mark the continent–ocean boundary. In the investigated area no seaward-dipping reflectors could be mapped, indicating that the rifting was not accompanied by the emplacement of massive subaerial volcanic sequences. Thus, we consider this margin as non-volcanic. This is in accordance with recent deep seismic results across the southern Yermak Plateau, where no evidence was found for the existence of a massive underplating of that region. No strong magnetic anomalies are identified between the Yermak Plateau and the continental margin of northern Svalbard.

ACKNOWLEDGMENTS

We are grateful for the excellent support of the captain and crew of the vessel RV *Polarstern*. Maps were produced using free software GMT (Wessel & Smith 1991). We thank two anonymous reviewers for their comments, which significantly improved the paper. This research has been partly funded by the Studienstiftung des Deutschen Volkes.

REFERENCES

Austegard, A. & Sundvor, E., 1991. The Svalbard continental margin: crustal structure from analysis of deep seismic profiles and gravity, *Seismo-Series*, **No. 53,** University of Bergen.

Bart, P.J. & Anderson, J.B., 1995. Seismic record of glacial events affecting the Pacific margin of the northwestern Antarctic Peninsula, in Geology and Seismic Stratigraphy of the Antarctic Margin, *Antarctic Research Series,* **68,** 74–95, eds Cooper, A.K., Barker, P.F., & Brancolini G., American Geophysical Union, Washington, DC.

Baturin, D.G., Fedukhina, T., Savostin, L. & Yunov, A., 1994. A geophysical survey of the Spitsbergen margin and surrounding areas, *Mar. geophys. Res.,* **16,** 463–484.

Butt, F.A., Elverhoi, A., Solheim, A. & Forsberg, C.F., 2000. Deciphering Late Cenozoic development of the western Svalbard Margin from ODP Site 986 results, *Mar. Geol.,* **169,** 373–390.

Červeny, V., Molotkov, I.A. & Pšenčik, I., 1977. *Ray Method in Seismology,* Charles University, Prague.

Cherkis, N.Z., Max, M.D., Vogt, P.R., Crane, K., Midthassel, A. & Sundvor, E., 1999. Large-scale mass wasting on the north Spitsbergen continental margin, Arctic Ocean, *Geo-Mar. Lett.,* **19,** 131–142.

Crane, K., Eldholm, O., Myhre, A.M. & Sundvor, E., 1982. Thermal implications for the evolution of the Spitsbergen Transform Fault, *Tectonophysics,* **89,** 1–32.

Czuba, W., Grad, M. & Guterch, A., 1999. Crustal structure of north-western Spitsbergen from DSS measurements, *Polish Polar Research,* **20/2,** 131–148.

Eiken, O., 1993. An Outline of the northwestern Svalbard continental margin, in *Arctic Geology and Petroleum Potential, Norsk Petrolium Forening Special Publication,* Vol. 2, pp. 619–629, eds Vorren, T.O., Bergsager, E., Dahl-Stamnes, O.A., Holter, E., Johansen, B., Lie, E. & Lund, T.B., Elsevier, Amsterdam.

Eiken, O., ed., 1994. Seismic Atlas of Western Svalbard: A selection of regional seismic transects, *Meddelelser,* Vol. 130, Norsk Polarinstitutt, Oslo.

Eiken, O. & Hinz, K., 1993. Contourites in the Fram Strait, *Sediment. Geol.,* **82,** 15–32.

Faleide, J.I., 1995. Free-air gravity field of the Northern Norwegian–Greenland Sea, in *Seafloor Atlas of the Northern Norwegian–Greenland Sea, Meddelelser,* Vol. 137, Plate 4, eds Crane, K. & Solheim, A., Norsk Polarinstitutt, Oslo.

Faleide, J.I., Solheim, A., Fiedler, A., Hjelstuen, B., Andersen, E.S. & Vanneste, K., 1996. Late Cenozoic evolution of the western Barents Sea–Svalbard continental margin, *Global and Planetary Change,* **12,** 53–74.

Feden, R.H., Vogt, P.R. & Fleming, H.S., 1979. Magnetic and bathymetric evidence for the 'Yermak Hot Spot' northwest of Svalbard in the Arctic Basin, *Earth planet. Sci. Lett.,* **44,** 18–38.

Fiedler, A. & Faleide, J.I., 1996. Cenozoic sedimentation along the southwestern Barents Sea margin in relation to uplift and erosion of the shelf, *Global and Planetary Change,* **12,** 75–93.

Forsberg, C.F., Solheim, A., Elverhoi, A., Jansen, E., Channell, J.E.T. & Andersen, E.S., 1999. The depositional environment of the western Svalbard margin during the late Pliocene and the Pleistocene: Sedimentary facies changes at Site 986, in *Proc. Ocean Drilling Program, Scientific Results,* Vol. 162, eds Raymo, M.E., Jansen, E., Blum, P. & Herbert, T.D., College station, TX.

Gardner, G.H.F., Gardner, L.W. & Gregory, A.R., 1974. Formation velocity and density—the diagnostic basics for stratigraphic traps, *Geophysics,* **39,** 770–780.

Harland, W.B., 1997. *The Geology of Svalbard,* Geol. Soc. Mem., **Vol. 17**.

Hellebrand, E., 2000. Petrology, in *The Expedition ARKTIS-XV/2 of 'Polarstern' in 1999, Berichte zur Polarforschung (Reports on Polar Research),* Vol. 368, pp. 59–70, ed. Jokat, W., Bremerhaven.

Hull, D.A., Osterman, L.E. & Thiede, J., 1996. Biostratigraphic Synthesis of Leg 151, North Atlantic-Arctic Gateways, in *Proc. Ocean Drilling Program, Scientific Results,* Vol. 151, pp. 627–644, eds Thiede, J., Myhre, A.M., Firth, J.V., Johnson, G.L. & Ruddiman, W.F., College station, TX.

IRIS, 2000. Incorporated Research Institutions for Seismology (IRIS), Data Management Center (DMC), Seattle, USA. http://www.iris.washington.edu/HTM/dms.htm.

Jackson, H.R., 2000. *Arctic Refraction Catalogue,* Geological Survey of Canada (Atlantic), Dartmouth, N.S., Canada. http://agcwww.bio.us.ca/pubprod/arctic/index.html.

Jackson, H.R., Johnson, G.L., Sundvor, E. & Myhre, A.M., 1984. The Yermak Plateau: formed at a triple junction, *J. geophys. Res.,* **89**(B5), 3223–3232.

Jakobsson, M., Cherkis, N.Z., Woodward, J., Macnab, R. & Coakley, B., 2000. New grid of the Arctic bathymetry aids scientists and mapmakers, *EOS, Trans. Am. geophys. Un.,* **81**, No. 9 (URL http://www.ngdc.noaa.gov/mgg/bathymetry/arctic.html).

Jokat, W., ed., 2000. The Expedition ARKTIS-XV/2 of 'Polarstern' in 1999, *Berichte zur Polarforschung (Reports on Polar Research),* **Vol. 368**, Alfred Wegener Institute, Bremerhaven.

Jokat, W., Weigelt, E., Kristoffersen, Y., Rasmussen, T. & Schöne, T., 1995. New insights into the evolution of the Lomonosov Ridge and the Eurasian Basin, *Geophys. J. Int.,* **122,** 378–392.

Jokat, W. *et al.*, 1999. Marine geophysics, in *Arctic'98: The Expedition ARK-XIV/1a of RV Polarstern in 1998, Berichte zur Polarforschung (Reports on Polar Research),* Vol. 308, pp. 14–25, ed. Jokat, W., Alfred Wegener Institute, Bremerhaven.

Jokat, W. *et al.*, 2002. Geophysical investigations, in *Polarstern Arktis XVII/2-Cruise Report: Amore 2001, Berichte zur Polarforschung (Reports on Polar Research),* Vol. 421, pp. 165–210, ed. Thiede, J., Alfred Wegener Institute, Bremerhaven.

Karasik, A.M., 1968. Magnetic anomalies of the Gakkel Ridge and origin of the Eurasia Subbasin of the Arctic Ocean, *Geophys. Methods Prospect. Arctic,* **5,** 8–19.

Karasik, A.M., 1974. The Eurasia Basin of the Arctic Ocean from the point of view of plate tectonics, in *Problems in Geology of Polar Areas of the Earth,* pp. 23–31, Nauchno-Issledovatelskiy Institut Geologii Arktiki, Leningrad (in Russian).

MacNab, R. & Verhoef, J., 1995. Magnetic Anomalies of the Northern Norwegian–Greenland Sea, in *Seafloor Atlas of the Northern Norwegian–Greenland Sea*, Meddelelser,Vol. 137, Plate 5, eds Crane, K. & Solheim, A., Norsk Polarinstitutt, Oslo.

Myhre, A.M., Eldholm, O. & Sundvor, E., 1982. The margin between Senja and Spitsbergen Fracture Zones: Implications from plate tectonics, *Tectonophysics,* **89,** 33–50.

Myhre, A.M., Thiede, J. & Firth, J., eds, 1995. Proc. Ocean Drilling Program, *Initial Reports,* Vol. 151, College station, TX.

Okay, N. & Crane, K., 1993. Thermal Rejuvenation of the Yermak Plateau, *Mar. geophys. Res.,* **15,** 243–263.

Okay, N., Crane, K., Vogt, P.R. & Sundvor, E., 1991. Thermal modelling of the Yermak Plateau within the Norwegian–Greenland Sea (Abs.), *EOS, Trans. Am. geophys. Un.,* **71,** 17,622.

Ritzmann, O. & Jokat, W., 2003. Crustal structure of northwestern Svalbard and the adjacent Yermak Plateau: Evidence for Oligocene simple shear rifting and non-volcanic break-up, *Geophys. J. Int.,* **152,** 139–159.

Shipboard Scientific Party, 1995a. Site 910, in *Proc. Ocean Drilling Program, Initial Reports,* Vol. 151, pp. 221–270, eds Myhre, A.M., Thiede, J. & Firth, J., College station, TX.

Shipboard Scientific Party, 1995b. Site 911, in *Proc. Ocean Drilling Program, Initial Reports,* Vol. 151, pp. 271–318, eds Myhre, A.M., Thiede, J. & Firth, J., College station, TX.

Sroda, P., 1999. *Modification to Software Package ZPLOT by C. Zelt (1998),* Polish Academy of Sciences, Warsaw.

Stein, R., Brass, G., Graham, D. Pimmel, A. & the Shipboard Scientific Party, 1995. Hydrocarbon measurements at the Arctic Gateways Sites (ODP Leg 151), in *Proc. Ocean Drilling Program, Initial Reports,* Vol. 151, pp. 385–395, eds Myhre, A.M., Thiede, J. & Firth, J., College station, TX.

Sundvor, E. & Austegard, A., 1990. The evolution of the Svalbard margins: Synthesis and new results, in *Geological History of the Polar Oceans: Arctic versus Antarctic,* Vol. 308, of NATO ASI Series C,

pp. 77–94, eds Bleil, U. & Thiede, J., Kluwer Academic Publishers, Dordrecht.

Sundvor, E., Gidskehaug, A., Myhre, A.M. & Eldholm, O., 1978. Marine Geophysical survey on the Northern Svalbard Margin, *Scientific Report,* No. 5, Seismological Observatory, University of Bergen.

Sundvor, E., Crane, K., Vogt, P.R., Martinez, F., Jones, C., deMoustier, C., Doss, H., Okay, N. & SeaMARC Team (A. Shor, M. Rognstad, S. Dong, D. Johnson & D. Bergensen), 1991. SeaMARC II and Associated Geophysical Investigation of the Knipovich Ridge, Molloy Ridge/Fracture Zone and Barents/Spitsbergen Continental Margin: Part I. Overview of Two Year Program Completed (Abs.), *EOS, Trans. Am. geophys. Un.,* **72,** 22,232.

Thiede, J., Myhre, A.M., Firth, J.V. & Shipboard Scientific Party, 1995. Cenozoic Northern Hemisphere polar and subpolar ocean paleoenvironments (Summary of ODP Leg 151 Drilling Results), in *Proc. Ocean Drilling Program, Initial Reports,* Vol. 151, pp. 397–420, eds Myhre, A.M., Thiede, J. & Firth, J., College station, TX.

Vogt, P.R., Taylor, P.T., Kovacs, L.C. & Johnson, G.L., 1979. Detailed aeromagnetic investigations of the Arctic Basin, *J. geophys. Res.,* **84,** 1071–1089.

Vogt, P.R., Bernero, C., Kovacs, L.C. & Taylor, P., 1981. Structure and plate tectonic evolution of the marine Arctic as revealed by aeromagnetics, 26th Internat. Geol. Cong., *Oceanol. Acta,* 4 SP, 25–40.

Weigelt, E., 1998. Die Krustenstruktur und Sedimentdecke des Eurasischen Beckens, Arktischer Ozean: Resultate aus seismischen und gravimetrischen Untersuchungen, *Berichte zur Polarforschung (Reports on Polar Research),* Vol. 261, Alfred Wegener Institute, Bremerhaven.

Wessel, P. & Smith, W.H.F., 1991. Free Software helps map and display data, *EOS, Trans. Am. geophys. Un.,* **72**, pp. 441, 445–446.

Zelt, C.A., 1998. *Zplot—an Interactive Plotting and Picking Program for Seismic Data*, Software manual (modified by P. Sroda, Warsaw 1999).

Zelt, C.A. & Smith, R.B., 1992. Seismic traveltime inversion for 2-D crustal velocity structure, *Geophys. J. Int.,* **108**, 16–34.